Assignment of Backbone Resonances in a Eukaryotic Protein Kinase – ERK2 as a Representative Example

ARTICLE *in* METHODS IN MOLECULAR BIOLOGY (CLIFTON, N.J.) · JANUARY 2012

Impact Factor: 1.29 · DOI: 10.1007/978-1-61779-480-3_19 · Source: PubMed

3 AUTHORS, INCLUDING:

Ranajeet Ghose
City College of New York
62 PUBLICATIONS **975** CITATIONS

SEE PROFILE

Published in final edited form as:
Methods Mol Biol. 2012 ; 831: 359–368. doi:10.1007/978-1-61779-480-3_19.

Assignment of Backbone Resonances in a Eukaryotic Protein Kinase – ERK2 as an Illustrative Example

Andrea Piserchio[1], **Kevin N. Dalby**[2,3], and **Ranajeet Ghose**[1,4]

[1]Department of Chemistry, The City College of New York, New York, NY 10031

[2]Division of Medicinal Chemistry, University of Texas, Austin, TX 78712

[3]Graduate Program in Pharmacy, University of Texas, Austin, TX 78712

[4]The Graduate Center of CUNY, New York, NY 10016

Summary

A first step towards the analysis of the structure, dynamics and interactions of proteins by NMR is obtaining an acceptable level of resonance assignments. This process is non-trivial in most eukaryotic kinases given their size and sub-optimal behavior in solution. Using inactive ERK2 as a representative example we describe the procedures we utilized to achieve a significant degree of completeness of backbone resonance assignment.

Keywords

MAP kinase; ERK2; TROSY; backbone resonance assignment; selective labeling; spin-labeled ATP

1. Introduction

ERK2 is a member of the extracellular signal-regulated kinase (ERK) sub-family of the mitogen activated protein kinases (MAPK). ERKs are upregulated in response to the activation of cell surface receptors mediated by extracellular cues such as hormones, cytokines and growth factors (1–3). ERKs play a central role in growth-factor related apoptosis in colorectal cancer (4), making the ERK signaling pathway a key target for cancer therapy (5, 6). The activation of ERKs (ERK1 and ERK2) occurs downstream of the Ras/Raf pathway upon dual phosphorylation of the conserved ^{183}Thr-X-Tyr^{185} motif by MEKKs (MAP/ERK kinase kinase) (7).

While the bacterial expression and purification of ERK2, at least in its inactive state focused on here, is more straightforward than some other eukaryotic kinases e.g. c-Src (see accompanying chapter in this volume, (8)), the complications in the NMR characterization due to the large size and extensive dynamics remain, a general trend in most eukaryotic kinases. A necessary step before NMR studies of structure, dynamics and interactions of these important signaling molecules can be undertaken is to obtain a sufficient number of assignments for backbone resonances. However, standard methodologies (9, 10) that are successful in smaller or better-behaved systems tend to fail for these important signaling molecules. This would explain the reason why only a few detailed NMR studies on eukaryotic kinases are available in the literature (11–15). Here we provide a description of

Address correspondence to: Ranajeet Ghose, Department of Chemistry, The City College of New York, 160 Convent Avenue, New York, NY 10031. Phone: (212) 650-6049; Fax: (212) 650-6107; rghose@sci.ccny.cuny.edu.

the procedures we applied to obtain resonance assignments for ERK2 These strategies illustrate how similar protocols can be utilized for other protein kinases. It is to be noted here, that generation of homogeneous samples of active dual phosphorylated (on Thr183 and Tyr185), active ERK2 for NMR studies is non-trivial and studies on the active, dual-phosphorylated species will be described elsewhere.

2. Assignment of Backbone Resonances for Full-length Inactive ERK2

The size of ERK2 (42 kDa), its tendency for non-specific aggregation at concentrations above approximately 200 μM, and dynamics on the slow to intermediate timescale leading to line-broadening effects, makes the assignment of backbone resonances quite non-trivial. Given these issues, the resonance assignment procedure for full-length inactive ERK2 in some detail, is described below.

2.1. Standard Triple Resonance Experiments

For inactive ERK2 (referred to as ERK2 from hereon forward), TROSY-based experiments (10, 16, 17) consistently displayed significantly narrower line widths, even at fields as low as 600 MHz, and were therefore preferred over their non-TROSY counterparts. However for samples prepared in D_2O-based media, the slow back exchange of several well-protected amide groups resulted in reduced sensitivity in backbone-directed NMR experiments complicating their analysis. This problem is evident when a $^{15}N,^{1}H$-TROSY spectrum of perdeuterated ERK2 (prepared in a D_2O-based medium) was compared to that of a sample prepared from cells grown in a $^{1}H_2O$-based medium supplemented with uniformly $^{2}H,^{15}N$-labeled amino-acids. The latter spectrum displayed additional sets of resonances not visible in the former. Incomplete back exchange complicates resonance assignment both by restricting the number of detectable resonances and by limiting the degree of correlations obtained (complicating the so-called backbone walk) for unambiguous correspondences between the resonances that are observed. This complication adds to the problem of the overall quality of the triple resonance experiments being poor, presumably because of the aforementioned aggregation phenomenon and dynamics. A TROSY-HNCO experiment collected at 800 MHz exhibits around 65–70% of the expected peaks. Clearly, this represents the upper limit for NMR assignment (for protein prepared in a D_2O-based medium where there is incomplete back-exchange of amide protons), given that HNCO is by far the most sensitive triple resonance experiment. In an HNCACB dataset collected at the same field and requiring a week of acquisition time, C^{β} (i-1) peaks were identified for approximately 43% of the expected resonances, if only the resonances also appearing in the HNCO experiment were considered (30% of the expected resonances considering the entire protein). Spectral overlap only partially justifies such an incomplete peak count. An HN(COCA)CB experiment collected at 600 MHz shows 53% of the spin systems visible in the HNCO (38% of the overall expected resonances). Fortunately, the C^{α}-based experiments were, by comparison, far more complete; the HN(CO)CA (also collected at 600 MHz), for example, includes 90% of the C^{α}(i-1) peaks expected from the HNCO-detected spin-systems. By combining this with an HNCA (collected at 800 MHz) experiment, most of the expected C^{α}(i), C^{α}(i-1) patterns matching the observed HNCO peaks could be successfully recognized. In addition, roughly 70% (relative to the HNCO-observed resonances) of the intra-residue HN(CA)CO peaks were also found. However, CO or C^{α}–based experiments are limited in scope since they allow the identification of only a limited number of amino-acid types unlike the C^{β}–based experiments. Clearly these statistics indicate that the extent of the NMR assignment achievable by using conventional approaches is fairly limited. Thus, we relied heavily on an approach that takes into consideration the structural and biochemical features of ERK2. A similar approach has been employed by Langer and coworkers (18) for assignment of the catalytic subunit of protein kinase A (PKA).

2.2. Use of Predicted Chemical Shifts

Several crystal structures of ERK2 can be found in the PDB, in both the inactive (19) and the dual-phosphorylated (on T183 and Y185) active (20) forms. A simple way to take advantage of the available structural data is to utilize them to predict the protein NMR chemical shifts. This can be done with reasonable accuracy for ^{13}C resonances, as long as the crystal structure reflects the structure in solution. Towards this purpose we used the software Sparta (21), freely available from Bax group. For well-ordered regions, like sheets and helices, these predictions are expected to be more accurate than for loops and regions of non-canonical secondary structure. Discrepancies may also be introduced in highly structured areas by the presence (or by the lack of) ligands or by intermolecular interactions either in solution (aggregation) or *in crystallo* (crystal-packing forces). The latter scenario is especially true in flexible and highly dynamic molecules (22, 23) as the protein kinases are known to be. It should be noted that in most of the crystal structures of ERK2 available in the PDB, it is in complex with a variety of ligands. In addition, the measured chemical shifts values are also affected by several sources of experimental error including those resulting from low digital resolution (especially for $^{13}C^{\beta}$), spectral overlap, poor signal to noise ratio and artifacts introduced due to pulse-sequence imperfections and non-idealities. We therefore used a relatively large cutoff (2.3 ppm) for differences between measured and predicted chemical shifts when evaluating a potential match for a ^{13}C resonance for a particular position along the protein sequence. Due to this large uncertainty and the large number of potential matches along the polypeptide chain, any comparison done at the level of individual residues leads to several ambiguous matches and is not particularly informative. If however, the comparison is done using stretches of three (or more) resonances peaks sequentially linked together, the method becomes much more useful. In particular we found that links typically of four, and sometimes three residues belonging to well-structured regions were sufficient to assign these resonances. We also found that, when analyzing areas of less well-defined secondary structure, this approach still remains useful when combined with the traditional analysis based on average chemical shifts values expected for a given residue type as obtained from the Biological Magnetic Resonance Data Bank (www.bmrb.wisc.edu). Often a link comprising four residues can be assigned to a protein loop if just three of the four residues in a given link correlate favorably to the corresponding predicted chemical shift values, provided that the chemical shifts observed for all four of them are compatible with the expected average database values of residues comprising the sequence.

2.3. Use of Structural Information

Clearly the assignments obtained using predicted chemical shifts should not be considered reliable until confirmed using more conventional experimental spectroscopy-based approaches. An obvious way to accomplish is to take advantage of the known three-dimensional structure of ERK2, and use the internuclear distances available from them for comparison with cross-peaks between amide protons that appear in a three-dimensional ^{15}N-edited NOESY-TROSY experiment. The verification of the existence (or the absence) of specific cross-peaks predicted from the crystal structure is an effective way to validate assignments, especially for β-strands and loops. In the case of β-sheets, the expected (and observed) NOEs are mainly long-range, allowing confirmation of sequentially non-proximal stretches of residues that comprise individual strands of a β-sheet that have been independently assigned. Certainly the reproduction of the proper patterns of internuclear distances from incorrectly assigned resonances would be highly unlikely. In case of loops, generally only few specific residues would be expected to be well structured and generate amide-amide NOEs, so again the observed NOE pattern can be used to confirm a tentative assignment. For helices however, the expected NOEs are mostly short range, and involves the amino acids in the helical segment, so they can be used principally to distinguish a

helical motif from a non-helical one. Inter-amide NOEs in helices can nevertheless be used as an aid to, or an alternative for, triple resonance experiments in order to sequentially link together the amino-acid spin systems. Since the early days of protein NMR spectroscopy when heteronuclear labeling was not commonplace, “walking” the sequential NH-NH NOEs represented a simple path to assign resonances corresponding to helical fragments (24). Furthermore, in samples of low proton density (as in the present case), spin-diffusion can be utilized to generate excellent medium range connectivities (i, i+2; i, i+3 etc) within helical stretches. For example, a ^{15}N-edited NOESY-TROSY experiment with a long mixing time (400 ms) effectively generates a TOCSY-like pattern among the NH resonances in a tight turn (Fig. 1). This process is greatly simplified by perdeuteration that reduces magnetization transfer to other regions of the protein. This is particularly useful in regions of spectral crowding, when resonance overlaps prevent the unambiguous identification of sequential NOEs at several positions.

2.4. Use of Selective Labeling Strategies

Selective amino acid labeling represents another route to aid the linking of neighboring spin systems and to fill gaps in assignments when the information content of the triple resonance experiments, especially in the C^{β} region, is poor. Usually, selective labeling (25) is performed by supplementing the M9 media with unlabeled (^{14}N) ammonium chloride, ^{1}H-^{12}C glucose, or similar nutrients (sometimes LB is used directly (26)), a particular ^{15}N labeled (^{15}N,^{12}C,^{1}H) amino acid, and sometimes an unlabeled (^{14}N,^{12}C,^{1}H) pool of the remaining amino acids. Then a simple ^{15}N,^{1}H HSQC experiment should highlight the amide resonances belonging to the residue type selected. This method can also be more rigorously applied using *E. coli* strains that are auxotrophic for the specific amino acid (27). Unfortunately this labeling approach did not perform well when applied to ERK2. Independently of the specific amino acid tested, the resulting HSQC spectrum lacked discernable peaks. We attributed this problem to extensive line broadening resulting from efficient ^{1}H-^{1}H relaxation in the absence of deuteration. Reducing the overall ^{1}H density by growing the bacteria in D_2O did not significantly improve the quality of the spectra suggesting that this was the result of the contribution of the local dipolar interactions between the amide and alpha protons of the selectively labeled amino acids. This would cause an increase in the contribution of the ^{1}H homonuclear R_1 to the relaxation rate of the antiphase term between the amide ^{15}N and ^{1}H nuclei, and would result in a broadening of the resonances in a ^{15}N,^{1}H-HSQC experiment. We then decided to alter our selective labeling approach and use amino-acids selectively ^{13}C-labeled only at the carbonyl position (^{14}N,^{12}C,^{13}CO,^{1}H) in a uniformly ^{15}N labeled, deuterated background. As shown by Takeuchi and coworkers (28), this ^{15}N labeled, deuterated background can be achieved by adding $^{15}NH_4Cl$ ^{12}C-^{2}H, glucose, and a pool of ^{15}N,^{12}C,^{2}H amino-acids (CELTONE base powder, Cambridge Isotope Laboratories) to the growth media, and by replacing H_2O with D_2O. HNCO experiments would then be expected to show peaks at a position corresponding to the selectively labeled carbonyl and the nitrogen of the following residue. While the alpha position of the labeled residues (i-1) is still protonated, the resonance detected corresponds to the amide ($^{1}H^{N}$) for the i^{th} residue that carries a deuteron at the C^{α} position. A further advantage of this approach is the higher resolution offered by the 3D HNCO compared to the extensive resonance overlap seen in 2D HSQC experiments used with the ^{15}N selective labeling approach. Another level of information provided by this labeling scheme is given by the disappearance of the resonances corresponding to the ^{14}N labeled amino acids (for those selectively ^{13}C-labeled at the carbonyl position) that can be monitored using 2D TROSY experiments. We successfully utilized this strategy for Gly, Ala, Leu, Val and Ile residues in ERK2 (representative examples are shown in Fig. 2).

2.5. Use of Spin-labeled ATP Analogs

Like all protein and indeed non-protein kinases, ERK2 binds ATP and ADP. However, the chemical shift perturbations induced by binding of these molecules (or corresponding slowly hydrolyzed analogs) are not limited to the ATP binding pocket, therefore the shifts of unknown resonances can be difficult to correlate to a specific portion of the structure simply by monitoring chemical shift perturbations. It has already been shown for PKA that spin-labeled ATP (sl-ATP) molecules can be successfully employed to highlight those residues within a certain distance from the binding pocket (18). The sl-ATP we employed, sl-N_3-ATP (a kind gift from Pia Vogel, SMU), carries a stable nitroxide spin-label as part of a 2,2,5,5 tetramethyl 3-pyrroline scaffold attached to the 3′ (70–80%) or 2′ (20–30%) positions of the ribose moiety (29). A crystal structure of ERK2 bound to this specific ligand does not exist, therefore we relied on the structure of ATP bound ERK2 (PDB: 1GOL) to estimate distances from the spin-label. We estimated that spin-labeled ATP in a ¼ (or ½) sub-stochiometric amount is capable of significantly quenching the HNCO peaks corresponding to residues within 20–25 Å of the 3′ ribose position (a representative example is shown in Fig. 3). Given the sub-stoichiometric amounts of sl-ATP used and the low affinity (30) of ATP for inactive ERK2 (K_D > ~700μM), the conformational changes induced by simple ATP binding are expected to be negligible. This approach helped extend the assignments in the area at the interface between the *N*- and *C*-lobes of ERK2, a critical region that was difficult to assign by other means. Using these strategies we have unambiguously assigned ~90 % (~65 % of all non-proline resonances) of the resonances seen/resolved at 800 MHz till date. The largest unassigned continuous stretch corresponds to the catalytic segment that can be expected to be in conformational exchange, a phenomenon that would lead to line-broadening effects. We are investigating alternative strategies to obtain assignments for this region including experiments that allow better visualization of exchange-broadened lines (31).

3. Conclusions

We focused on the problem of the NMR backbone assignment of eukaryotic kinases, using ERK2 as an example. NMR studies of this class of proteins is hindered by a number of problems, namely incomplete amide protons back exchange, aggregation/oligomerization at high protein concentration and internal dynamics. We have shown here that the careful analysis of otherwise well-established NMR experiments that can be normally found in most standard pulse sequence libraries can lead an acceptable level of resonance assignment. However, this process requires multiple sample conditions (different ligands, selectively labeled samples, spin-labeled ATP etc.) and available structural information. In general, we have found that the resonance assignment of the sites of protein-protein interactions (where known, as in ERK2) is significantly less challenging than the highly dynamic regions around the catalytic site. This process of resonance assignment is certainly time and resource consuming but is clearly worthwhile given the medical importance of these signaling molecules.

Acknowledgments

This research has been supported by the following grants from the National Institutes of Health: GM084278 (to RG), GM059802 (to KND) and 5G12 RR03060 (towards partial support of the NMR facilities at The City College of New York). RG is a member of the New York Structural Biology Center, NYSTAR facility. KND is a recipient of a grant from the Welch Foundation (F-1390). The authors thank Dr. Pia Vogel (SMU) for the kind gift of spin-labeled ATP.

References

1. Murphy LO, Blenis J. MAPK signal specificity: the right place at the right time. Trends Biochem Sci. 2006; 31:268–275. [PubMed: 16603362]
2. Chen Z, Gibson TB, Robinson F, Silvestro L, Pearson G, Xu B, Wright A, Vanderbilt C, Cobb MH. MAP kinases. Chem Rev. 2001; 101:2449–2476. [PubMed: 11749383]
3. Pearson G, Robinson F, Beers Gibson T, Xu BE, Karandikar M, Berman K, Cobb MH. Mitogen-activated protein (MAP) kinase pathways: regulation and physiological functions. Endocrine Rev. 2001; 22:153–183. [PubMed: 11294822]
4. Fang JY, Richardson BC. The MAPK signalling pathways and colorectal cancer. The Lancet Oncol. 2005; 6:322–327.
5. Kohno M, Pouyssegur J. Targeting the ERK signaling pathway in cancer therapy. Annal Med. 2006; 38:200–211.
6. Kohno M, Pouyssegur J. Pharmacological inhibitors of the ERK signaling pathway: application as anticancer drugs. Prog Cell Cyc Res. 2003; 5:219–224.
7. Roux PP, Blenis J. ERK and p38 MAPK-activated protein kinases: a family of protein kinases with diverse biological functions. Microbiol Mol Biol Rev. 2004; 68:320–344. [PubMed: 15187187]
8. Piserchio A, Dalby KN, Ghose R. Expression and Purification of Src-family Kinases for Solution NMR Studies. Meth Mol Biol. 2011 submitted.
9. Sattler M, Schleucher J, Griesinger C. Heteronuclear multidimensional NMR experiments for the structure determination of proteins in solution employing pulsed field gradients. Prog NMR Spectr. 1999; 34:93–158.
10. Salzmann M, Pervushin K, Wider G, Senn H, Wuthrich K. TROSY in triple-resonance experiments: new perspectives for sequential NMR assignment of large proteins. Proc Natl Acad Sci USA. 1998; 95:13585–13590. [PubMed: 9811843]
11. Masterson LR, Mascioni A, Traaseth NJ, Taylor SS, Veglia G. Allosteric cooperativity in protein kinase A. Proc Natl Acad Sci USA. 2008; 105:506–511. [PubMed: 18178622]
12. Masterson LR, Cheng C, Yu T, Tonelli M, Kornev A, Taylor SS, Veglia G. Dynamics connect substrate recognition to catalysis in protein kinase A. Nature Chem Biol. 2010; 6:821–828. [PubMed: 20890288]
13. Wiesner S, Wybenga-Groot LE, Warner N, Lin H, Pawson T, Forman-Kay JD, Sicheri F. A change in conformational dynamics underlies the activation of Eph receptor tyrosine kinases. EMBO J. 2006; 25:4686–4696. [PubMed: 16977320]
14. Vajpai N, Strauss A, Fendrich G, Cowan-Jacob SW, Manley PW, Grzesiek S, Jahnke W. Solution conformations and dynamics of ABL kinase-inhibitor complexes determined by NMR substantiate the different binding modes of imatinib/nilotinib and dasatinib. J Biol Chem. 2008; 283:18292–18302. [PubMed: 18434310]
15. Vogtherr M, Saxena K, Hoelder S, Grimme S, Betz M, Schieborr U, Pescatore B, Robin M, Delarbre L, Langer T, Wendt KU, Schwalbe H. NMR characterization of kinase p38 dynamics in free and ligand-bound forms. Angew Chem Intl Ed Engl. 2006; 45:993–997.
16. Riek R, Pervushin K, Wuthrich K. TROSY and CRINEPT: NMR with large molecular and supramolecular structures in solution. Trends Biochem Sci. 2000; 25:462–468. [PubMed: 11050425]
17. Pervushin K. Impact of transverse relaxation optimized spectroscopy (TROSY) on NMR as a technique in structural biology. Q Rev Biophys. 2000; 33:161–197. [PubMed: 11131563]
18. Langer T, Vogtherr M, Elshorst B, Betz M, Schieborr U, Saxena K, Schwalbe H. NMR backbone assignment of a protein kinase catalytic domain by a combination of several approaches: application to the catalytic subunit of cAMP-dependent protein kinase. ChemBioChem. 2004; 5:1508–1516. [PubMed: 15481030]
19. Zhang F, Strand A, Robbins D, Cobb MH, Goldsmith EJ. Atomic structure of the MAP kinase ERK2 at 2.3 Å resolution. Nature. 1994; 367:704–711. [PubMed: 8107865]
20. Canagarajah BJ, Khokhlatchev A, Cobb MH, Goldsmith EJ. Activation mechanism of the MAP kinase ERK2 by dual phosphorylation. Cell. 1997; 90:859–869. [PubMed: 9298898]

21. Shen Y, Bax A. Protein backbone chemical shifts predicted from searching a database for torsion angle and sequence homology. J Biomol NMR. 2007; 38:289–302. [PubMed: 17610132]
22. Fushman D, Xu R, Cowburn D. Direct determination of changes of interdomain orientation on ligation: use of the orientational dependence of ^{15}N NMR relaxation in Abl SH(32). Biochemistry. 1999; 38:10225–10230. [PubMed: 10441115]
23. Piserchio A, Nair PA, Shuman S, Ghose R. Solution NMR studies of Chlorella virus DNA ligase-adenylate. J Mol Biol. 2010; 395:291–308. [PubMed: 19913033]
24. Wüthrich, K. NMR of proteins and nucleic acids. John Wiley and Sons; New York: 1986.
25. Muchmore DC, McIntosh LP, Russell CB, Anderson DE, Dahlquist FW. Expression and nitrogen-15 labeling of proteins for proton and nitrogen-15 nuclear magnetic resonance. Meth Ezymnol. 1989; 177:44–73.
26. Englander J, Cohen L, Arshava B, Estephan R, Becker JM, Naider F. Selective labeling of a membrane peptide with ^{15}N-amino acids using cells grown in rich medium. Biopolymers. 2006; 84:508–518. [PubMed: 16741986]
27. LeMaster DM, Cronan JE Jr. Biosynthetic production of ^{13}C-labeled amino acids with site-specific enrichment. J Biol Chem. 1982; 257:1224–1230. [PubMed: 7035446]
28. Takeuchi K, Ng E, Malia TJ, Wagner G. 1-^{13}C amino acid selective labeling in a ^{2}H^{15}N background for NMR studies of large proteins. J Biomol NMR. 2007; 38:89–98. [PubMed: 17390105]
29. Vogel-Claude P, Schafer G, Trommer WE. Synthesis of a photoaffinity-spin-labeled derivative of ATP and its first application to F1-ATPase. FEBS Lett. 1988; 227:107–109. [PubMed: 2892696]
30. Prowse CN, Lew J. Mechanism of activation of ERK2 by dual phosphorylation. J Biol Chem. 2001; 276:99–103. [PubMed: 11016942]
31. Li Y, Palmer AG III. Narrowing of protein NMR spectral lines broadened by chemical exchange. J Am Chem Soc. 2010; 132:8856–8857. [PubMed: 20550111]

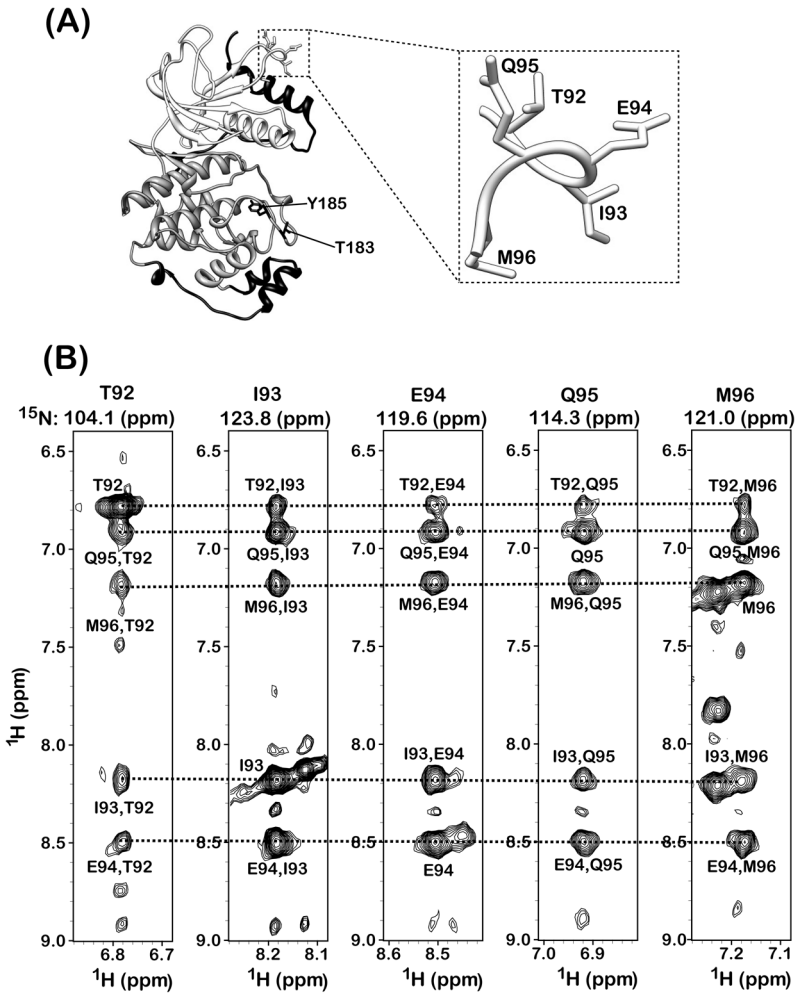

Figure 1.

(A) Structure of ERK2 with the *N*- and *C*-terminal lobes colored light and dark-grey respectively. The MAP kinase insert and the *C*-terminal extension are colored black. Side-chains for the regulatory T183 and Y185 residues are shown and labeled. Side-chains for the tight turn encompassing residues T92-M96 are shown on the structure and expanded on the right panel. **(B)** Strips taken from a ^{15}N-edited NOESY-TROSY spectrum collected with a 400 ms mixing time at 800 MHz on a uniformly ^{2}H,^{13}C,^{15}N-labled inactive ERK2 sample in a buffer containing 150 m*M* NaCl, 2 m*M* DTT, 10 m*M* $MgCl_2$, 2 m*M* ADP, 50 m*M* phosphate, pH 6.8, 10 % $^{2}H_2O$. Shown here is the effect of spin diffusion generating long-range connections among the amides of the segment comprising of residues T92-M96. The lines highlight the total correlation-like (as in a TOCSY experiment where transfer occurs through scalar rather than dipolar couplings) effect of the magnetization transfer. The source (first label) and target (last label) amide $^{1}H^{N}$ nuclei for the cross-peaks are labeled. Only a single label is used for the diagonal peaks.

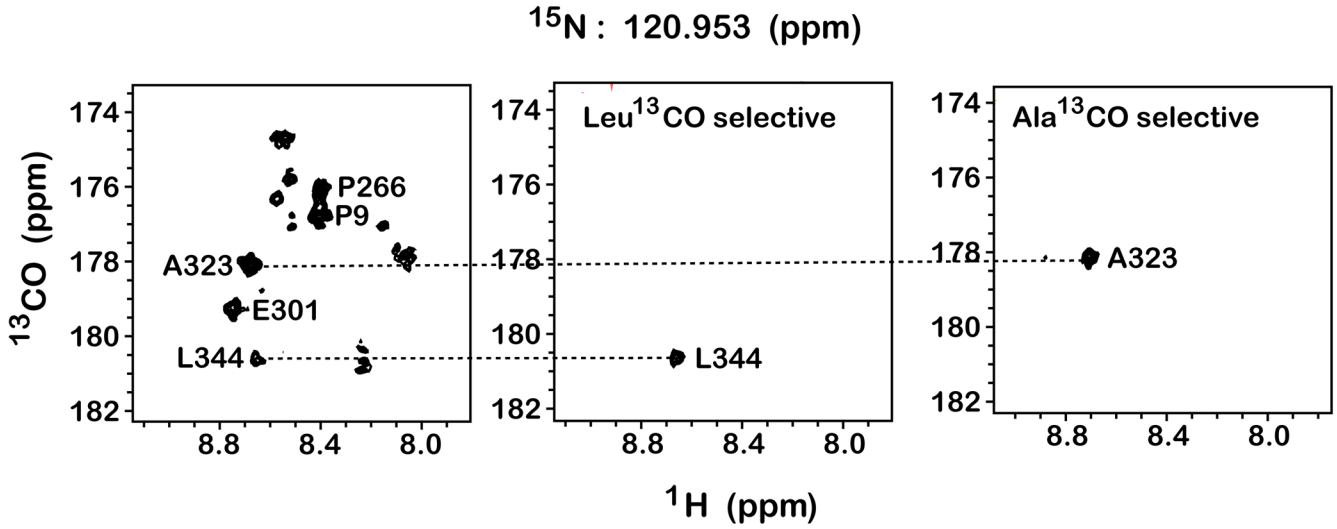

Figure 2.
^{13}CO, ^{1}H planes for TROSY-based HNCO spectra for representative examples (Leu, Ala) of residue-selective ^{13}CO labeled samples of ERK2 in a uniformly ^{5}N-labeled, per-deuterated background. Also shown in the extreme left panel, is the corresponding plane from uniformly ^{13}C,^{2}H,^{15}N-labeled ERK2. The labels correspond to the residue that contributes the ^{13}CO nucleus (i.e. the i-1 residue).

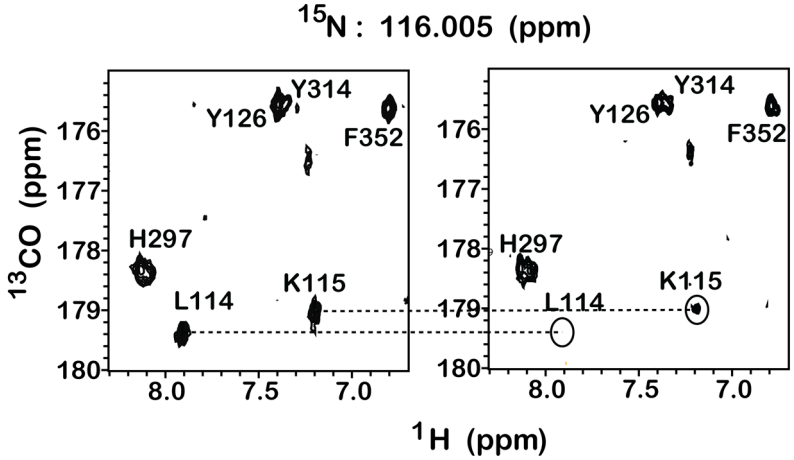

Figure 3.

Paramagnetic relaxation enhancement (PRE) monitored using TROSY-based HNCO experiments. Partial and complete quenching for L114 and K115, respectively, induced by sub-stoichiometric amount of sl-ATP (1:0.25 ratio) are illustrated. Both residues are a distance of around ~12 Å from the label.